

Supporting Information

Thermoplastic Nanofluidic Devices for Identifying Abasic Sites in Single DNA Molecules

Swarnagowri Vaidyanathan,^{1,6, φ} Kumuditha M. Weerakoon-Ratnayake,^{2,6, φ} Franklin I. Uba,⁴ Bo Hu,⁵ David Kaufman,^{6,7} Junseo Choi,^{6,8} Sunggook Park,^{6,8} Steven A. Soper^{1,2,6,9*}

¹*Bioengineering Program, The University of Kansas, Lawrence, KS 66045 USA*

²*Department of Chemistry, The University of Kansas, Lawrence, KS 66045 USA*

³*Department of Mechanical Engineering, The University of Kansas, Lawrence, KS 66045 USA*

⁴*Department of Chemistry, University of North Carolina at Chapel Hill, NC 27599 USA*

⁵*Department of Biomedical Engineering, The University of North Carolina at Chapel Hill, Chapel Hill, NC 27599 USA*

⁶*Center of BioModular Multiscale Systems for Precision Medicine, Lawrence, KS 66047 USA*

⁷*Department of Pathology and Laboratory Medicine, The University of North Carolina at Chapel Hill, Chapel Hill, NC 27599 USA*

⁸*Department of Mechanical Engineering, Louisiana State University, Baton Rouge, LA 70810 USA*

⁹*Department of Cancer Biology and KU Cancer Center, The University of Kansas Medical Center, Kansas City, KS 66106 USA*

φAuthors contributed equally

*Corresponding Author: ssoper@ku.edu

Keywords: Nanofluidics, single-molecule detection, DNA Abasic Sites

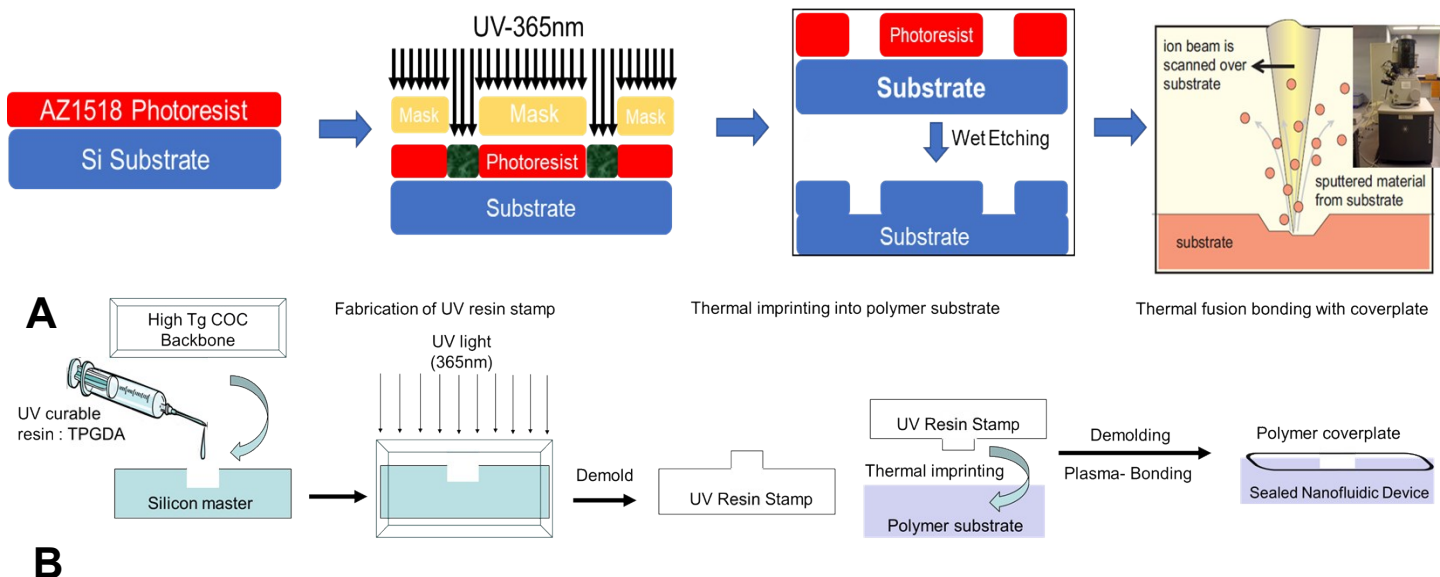


Figure S1. Schematic showing the top down fabrication process used to make the plastic nanofluidic devices used in these studies. **(A)** First, photolithography on Si wafer using AZ1518 resist was performed followed by wet etching to achieve the desired depth of the microfluidic channels. As a final step, FIB was performed to fabricate the nanodimensional features on the Si master. **(B)** The NIL steps are shown here. Briefly, the features from the Si master were transferred to a resin stamp using UV light. They were then thermally imprinted using NIL into a PMMA substrate. Finally, thermal fusion bonding was performed to seal the fluidic network with a COC cover plate.

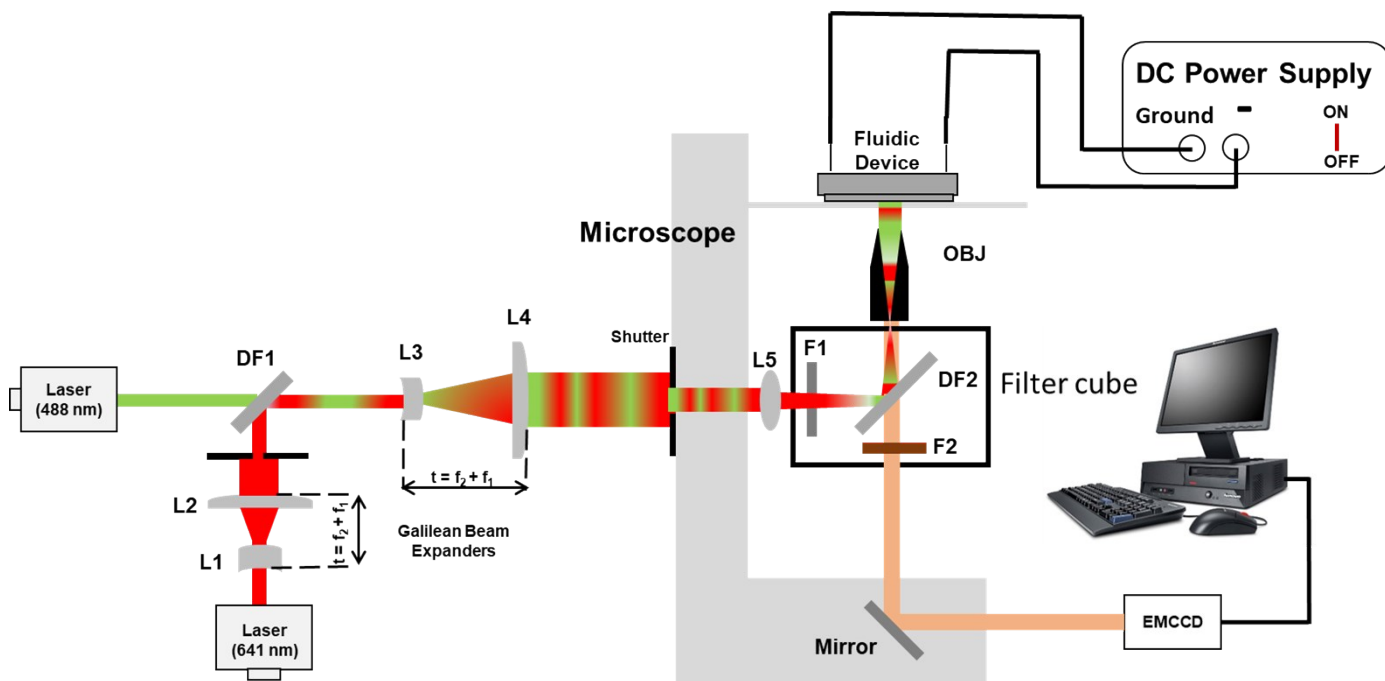


Figure S2. Schematic of the dual-color microscope system for single-molecule tracking and imaging. The nanofluidic device was placed on a translational stage associated with the inverted microscope and Pt electrodes were placed within specific reservoirs of the chip to supply the driving electric field to the chip using a DC power supply, which was earth grounded. Switching between the two lasers was controlled manually with a 1 s switching delay using a filter cube resident within the microscope. All images were acquired using an EMCCD camera and Metamorph software.

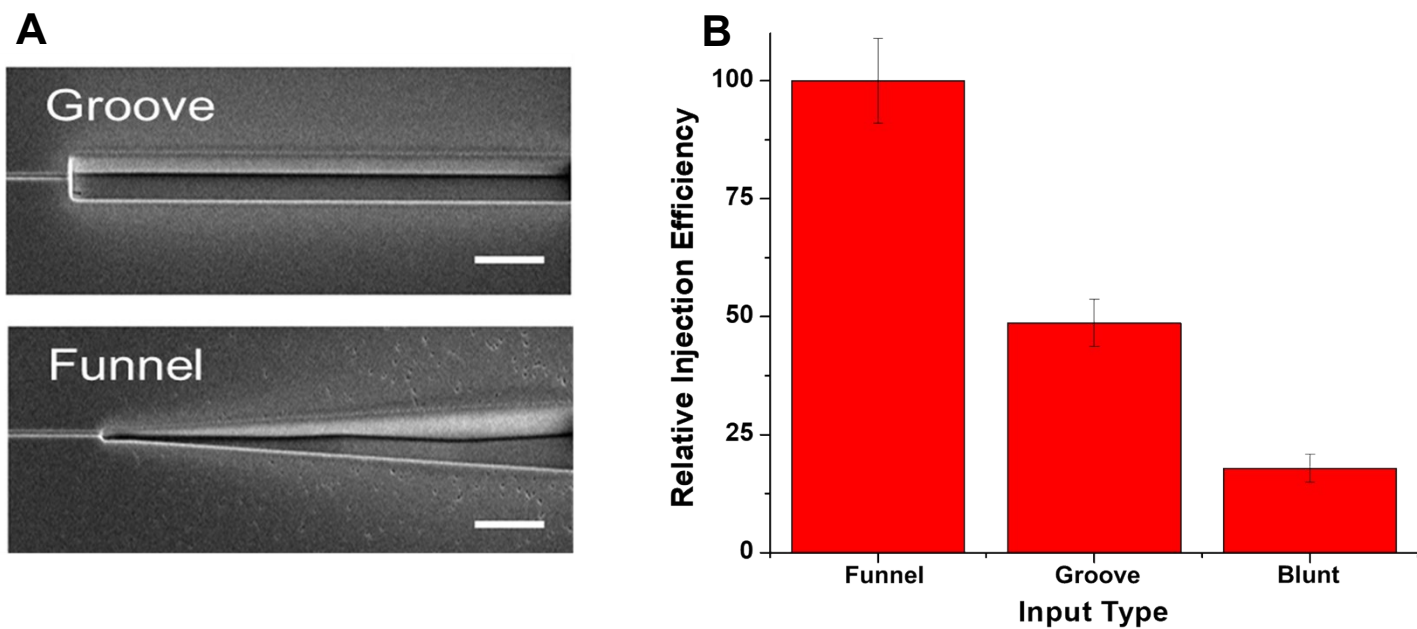
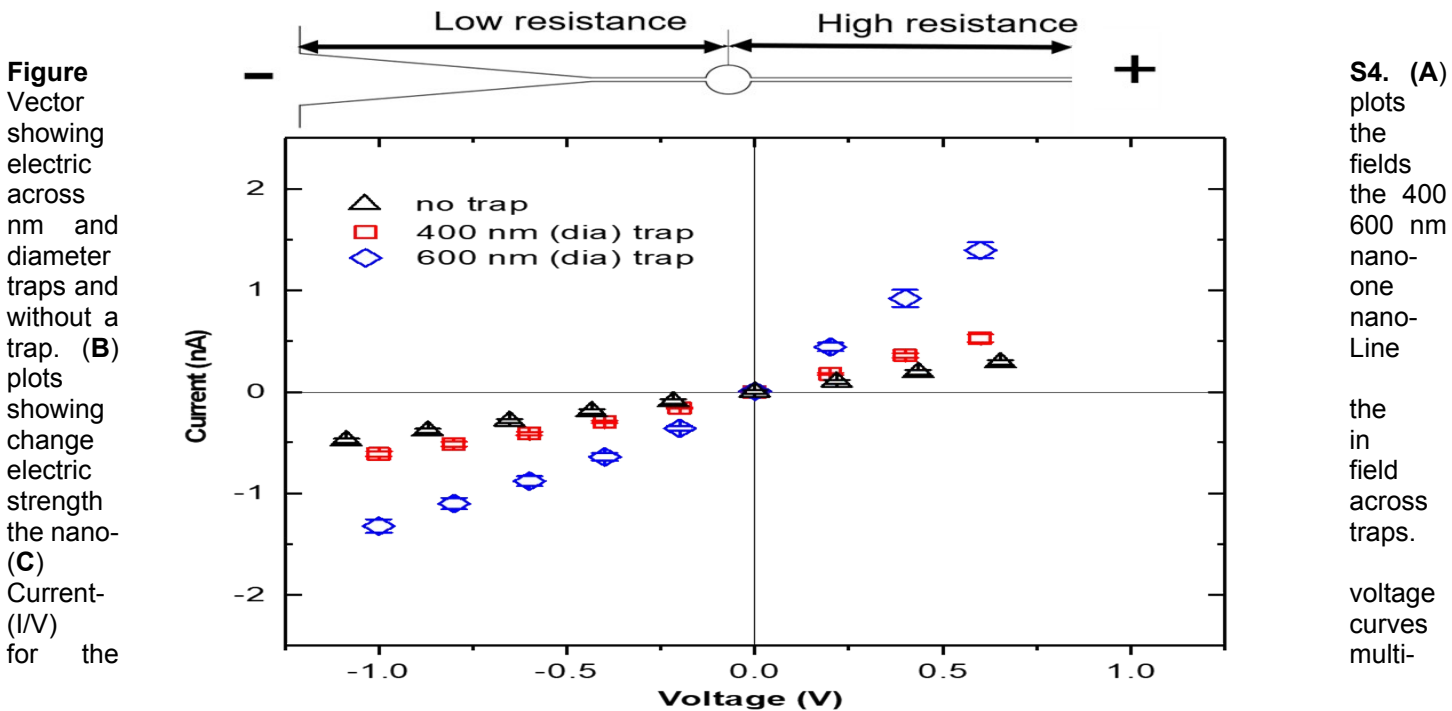
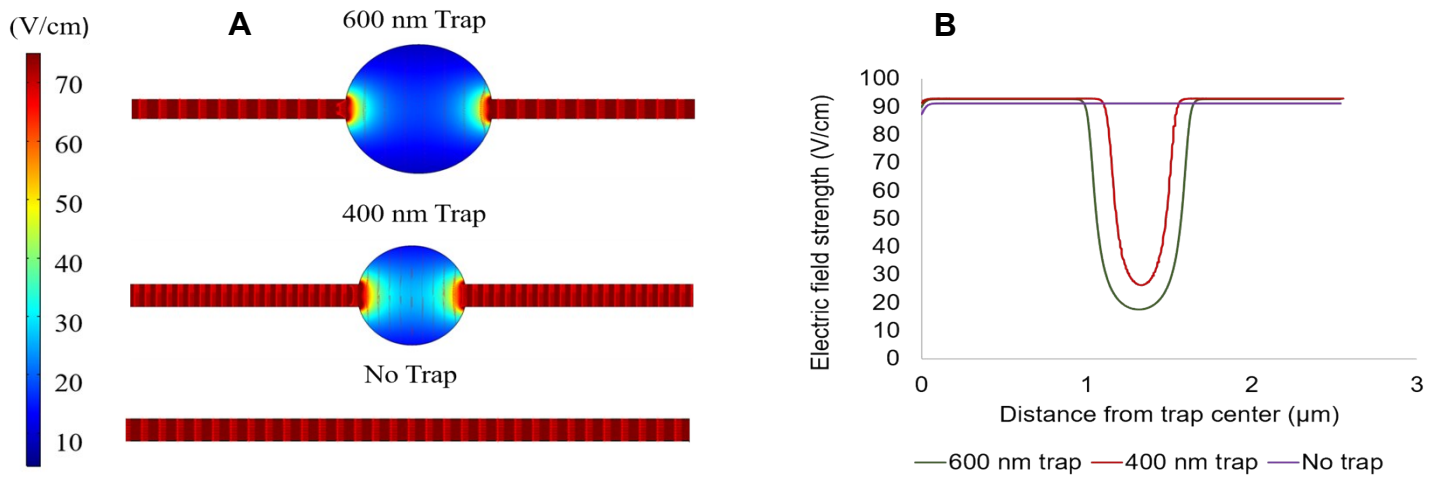


Figure S3. (A) SEMs of two input types used to interface the nanofluidic network to the access microchannels. In these SEMs are shown the Funnel and Groove inputs. The white scale bars represent 500 nm. The nanochannel shown on the left is 100 nm x 80 nm (width x depth). (B) Relative injection efficiency (%) of λ -DNA (48.5 Kbp) into the nanofluidic circuit for three types of nanochannel/microchannel interfaces. For the Blunt input type, the access microchannel of the device was directly connected to the nanofluidic channel. All data were normalized with respect to the Funnel input event frequency.

COMSOL analysis of the nano-trap. COMSOL simulations were performed to investigate the effects of trap size on the electric field distribution and on the translocation rate of dsDNA. When a voltage of 0.1 V was applied to the nanofluidic circuit, dsDNA entered into the 3D funnel from the microchannel and then into the nano-trap. We speculated that the trap size would influence the trapping and translocation rates of dsDNA molecules. Figure S4A shows COMSOL simulation results for the electric field strength distribution within two different sized nano-traps (assumed a cylindrical geometry). The 600 nm trap had a field drop of ~ 70 V/cm from the feeding nanochannel to the center of the nano-trap (see Figure S4B), whereas the smaller 400 nm trap showed a drop of ~ 55 V/cm. Thus, it would be expected that the effective field strength influencing the DNA molecules inside the nano-trap was higher in the smaller nano-trap (400 nm) and thus, would require less driving voltage to eject a molecule from this trap compared to the larger nano-trap. Typically, concentration polarization is exhibited in channel dimensions less than <50 nm when a low ionic strength buffer is used and because of this, the field distribution may be different from what is shown in Figure S4 due to changes in the zeta potential. However, concentration polarization requires significant overlap in the electrical double layer, EDL.¹⁻⁴ In our experiments and simulations, we did not experience significant EDL overlap as the buffer used was 1X TBE (89 mM Tris, 89 mM borate, 2 mM EDTA), generated an EDL thickness of 1.3 nm,⁵ and the smallest channels used in our nanofluidic circuit was 80 x 110 nm, which indicated that EDL overlap was $<2\%$.

The current voltage (I/V) characteristics were measured for devices without and with nano-traps of different sizes. From Figure S4C for the same applied voltage, different I/V curves were obtained for devices with different trap sizes. Two main factors contribute to the rectification of the ionic current in the nanofluidic circuit, which

were due to asymmetry in either the geometry of the channel network or surface charge.⁶ Here, we treated the entire device with an O₂ plasma to facilitate thermal fusion bonding, and hence, the surface charge was assumed to be symmetric throughout the circuit (for a fully deprotonated PMMA nanochannel, the surface charge is -40.5 mC/m²).⁷ However, the presence of the inlet funnel and the nano-trap followed by the stretching nanochannels made the nanofluidic circuit geometry asymmetric. Hence, the presence of a larger nano-trap increased the ion selectivity ratio between the nanochannel (shallow region) and the nano-trap (deep region), which increased the rectification and thus, a more non-linear IV plot.^{6, 8}



structured nanofluidic circuit with no nano-trap (black), 400 nm (red) and 600 nm diameter (blue) nano-traps measured with 1 M KCl added to 1X TBE buffer (pH = 8.0). Each data point represents the mean \pm standard deviation from five different measurements. One M KCl was spiked into the buffer to increase the current flowing through the device.

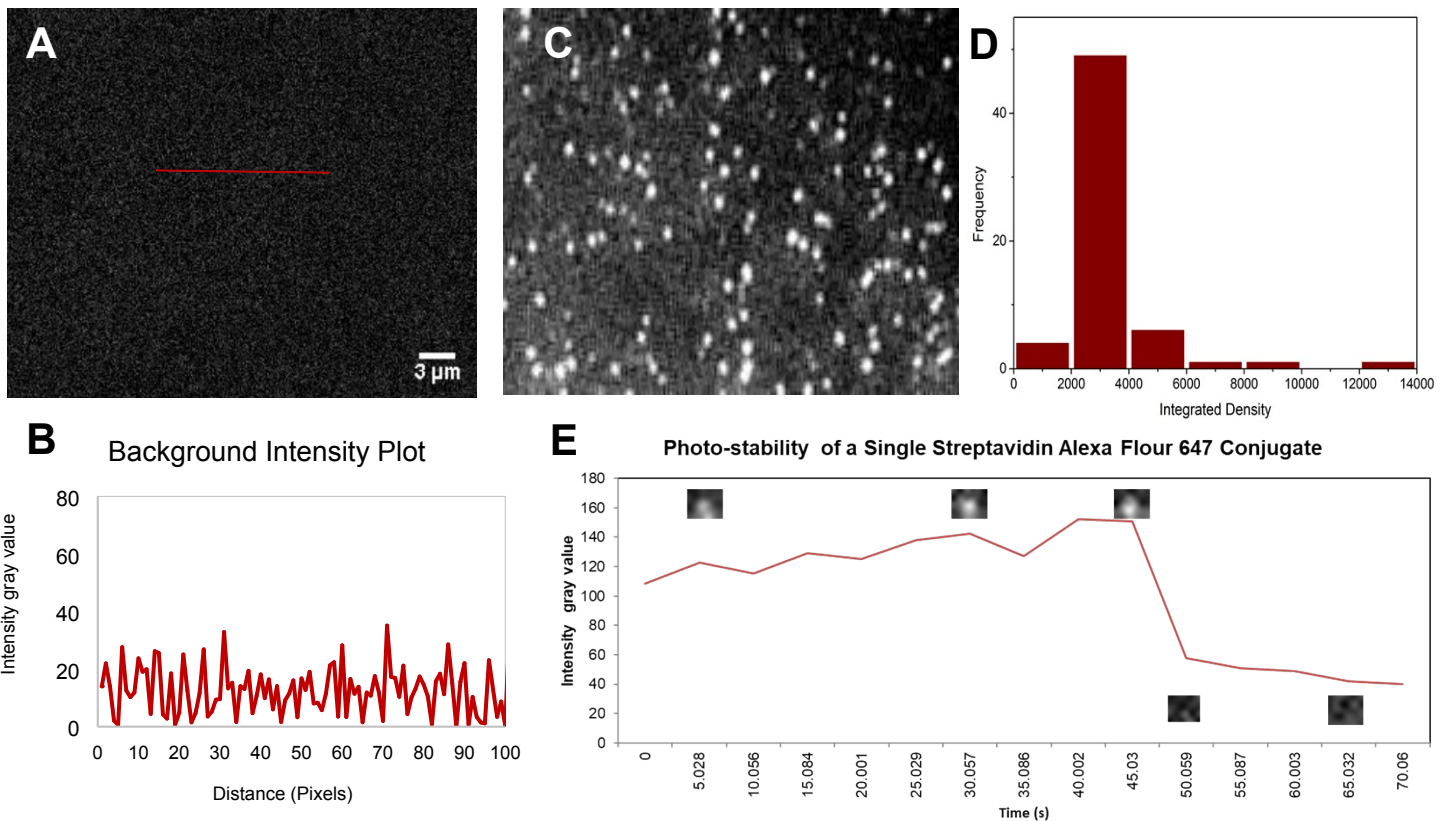
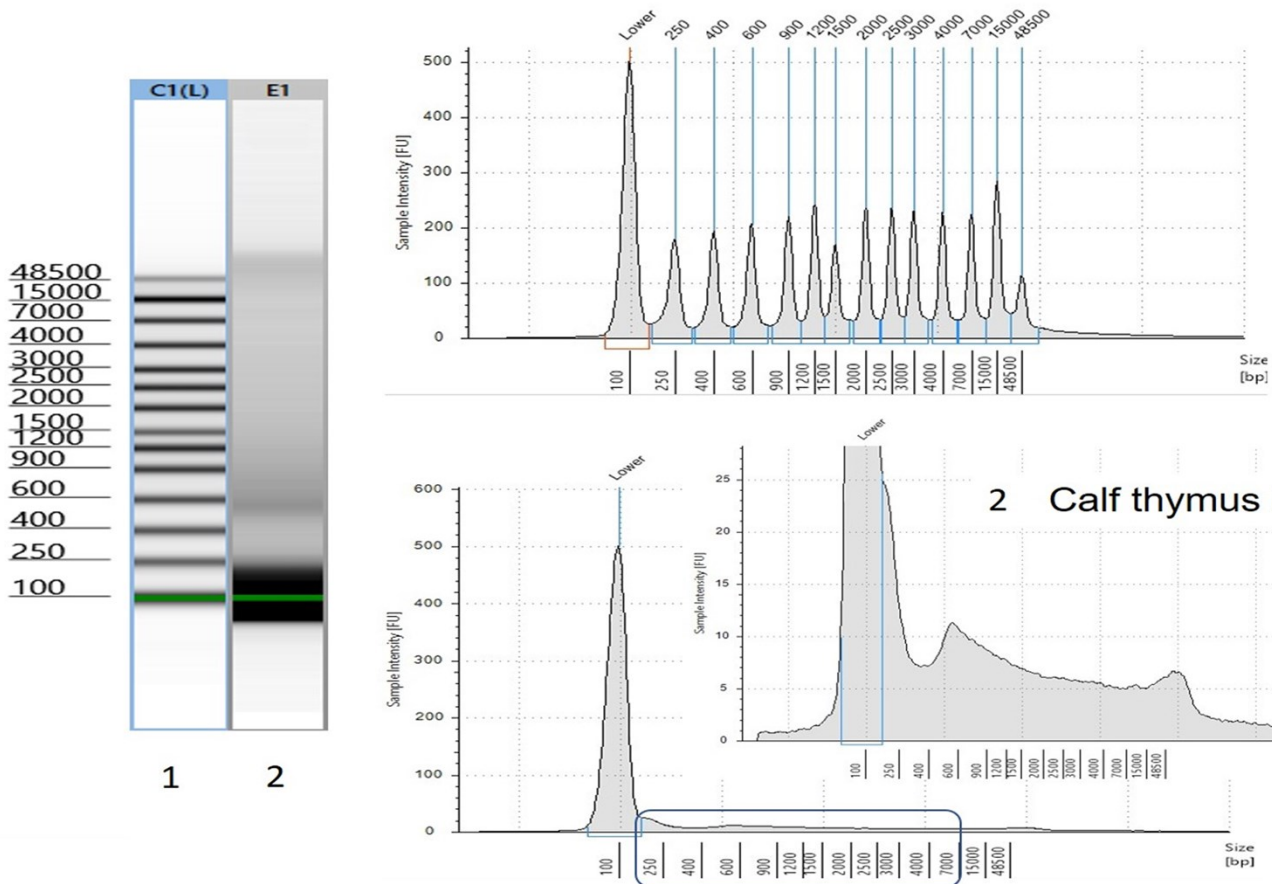


Figure S5. (A) Background image to evaluate the noise and speckle pattern imaged from a COC cover plate. (B) Line plot showing background intensity gray values. (C) Images of streptavidin Alexa Fluor 647 conjugates deposited on a COC cover plate. Excitation was provided by the 641 nm red laser with the fluorescence collected using a 100X (1.49 N/A) microscope objective. (D) Histograms showing the number of occurrences (frequency) for integrated intensity of all current voxels for single fluorescently labeled streptavidin molecules. (E) The bleaching of a streptavidin molecule at various time points and the corresponding intensity gray values. The sharp intensity drop at around 45.03 s corresponds to a single-molecule bleaching event.

Dual-color single-molecule imaging/tracking microscope. Characterization of the dual colored laser microscope system was undertaken to ensure its suitability for imaging single molecules using the red laser, which was used to image AP sites in a dsDNA molecule. The background was analyzed for its intensity values and speckle pattern. From Figures S5A-B, it can be seen that the background noise and speckle corresponded to an intensity value of ~30. This value was found to be consistent throughout the imaging area. Next, 0.2 μ L of streptavidin-labeled Alexa Fluor 647 nm dye molecules were placed on a COC cover plate and imaged using a 100X oil immersion objective (1.49 NA). The fluorescence was measured using an EMCCD camera. Figure S5C shows the presence of individual spots, which corresponded to Alexa Fluor dye molecules attached to streptavidin that were of significantly higher intensity compared to the background signal. Upon magnification of the individual spots, we found that each spot spread over a 3 X 3 pixel array, which occupied a larger pixel area compared to the speckles shown in Figure S5A. The total integrated density of the 3 X 3 pixel array for each spot was measured and the integrated intensity values are plotted as a bar graph in Figure S5D. The streptavidin molecules were continuously irradiated and the intensity was followed over a period of 70 s as shown in Figure S5E. As can be seen, a sudden drop in the intensity was observed at around 45 s, which indicated a bleaching event for a single molecule.

1 Ladder



2 Calf thymus DNA

Figure S6. Tape station data for abasic site labeled Calf-thymus DNA from the Dojindo abasic site quantification kit. According to the data, there are various lengths of DNA strands present in the sample.

DNA fragment size for calf-thymus DNA. In order to obtain the size of the calf-thymus DNA, the DNA was run using a TapeStation gel electrophoresis system to determine accurately the bp length. From Figure S6, it can be seen that there was not a fixed length of DNA, but rather a distribution of different lengths. The sizes of the DNA fragments ranged from 250 bp to 48,500 bp. Therefore, every fiber that was analyzed was considered individually when extended in the stretching nanochannel using the intercalating dye for DNA visualization. Following DNA length measurements, the corresponding AP sites were scored and normalized to 10^5 bp of dsDNA.

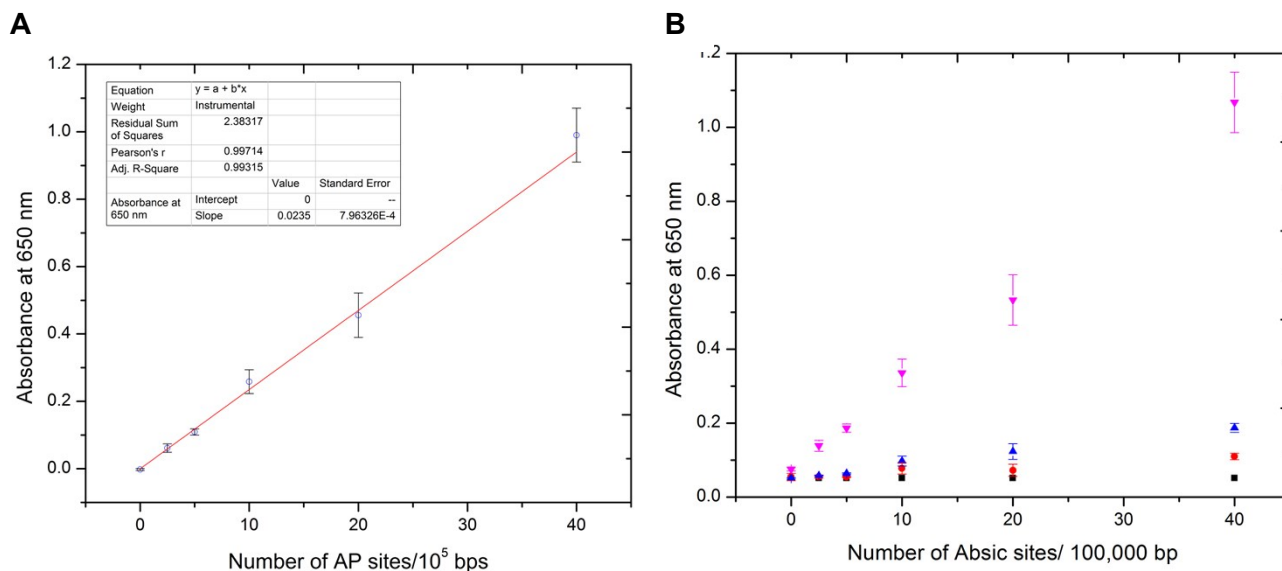


Figure S7. (A) Calibration curve for a colorimetric assay for measuring AP sites in dsDNA. The data was collected by measuring absorbance at 650 nm in a 96-well plate reader. Data points were obtained using 3 duplicate measurements and fitted to a linear calibration curve, which yielded a correlation coefficient of 0.997. **(B)** Calibration data points using the colorimetric assay based on a 96-well plate for different concentrations of dsDNA. Controls with no abasic DNA are shown in black and different concentrations of abasic dsDNA are shown in red (0.025 ng/ μ L), blue (0.075 ng/ μ L), and pink (0.300 ng/ μ L) with respect to the number of AP sites per unit length of dsDNA.

Benchmark determination of AP site frequency. The standard AP site colorimetric assay from Dojindo Molecular Technologies was used to measure the number of abasic sites in the DNA by measuring absorbance at 650 nm. The detailed procedure can be found in their website. Briefly, genomic calf-thymus DNA with AP sites (0, 2.5, 5, 10, 20, 40 AP sites/ 10^5 bp) were reacted with the Aldehyde Reactive Probe (ARP), filtered using a column, and bound to the wells of a 96-well plate and labelled with HRP streptavidin. As seen in Figure S7A, the absorbance was measured and based on the values obtained, the number of AP sites were obtained. We further reduced the concentration from the standard (0.300 ng/ μ L) to 0.075 ng/ μ L, 0.025 ng/ μ L, and a control (no AP sites) and repeated the same measurements. From Figure S7B, we noted that at lower concentrations, the calorimetric method did not accurately measure the number of AP sites due to SNR considerations.

References:

1. S. J. Kim, Y.-C. Wang, J. H. Lee, H. Jang and J. Han, *Physical Review Letters*, 2007, **99**, 044501.
2. S. J. Kim, L. D. Li and J. Han, *Langmuir*, 2009, **25**, 7759-7765.
3. A. Plecis, R. B. Schoch and P. Renaud, *Nano Letters*, 2005, **5**, 1147-1155.
4. R. Dhopeswarkar, R. M. Crooks, D. Hlushkou and U. Tallarek, *Analytical Chemistry*, 2008, **80**, 1039-1048.
5. S.-S. Hsieh, H.-C. Lin and C.-Y. Lin, *Colloid Polym Sci*, 2006, **284**, 1275-1286.
6. M. A. Alibakhshi, B. Liu, Z. Xu and C. Duan, *Biomicrofluidics*, 2016, **10**, 054102.
7. F. I. Uba, S. Pullagurra, N. Sirasunthorn, J. Wu, S. Park, R. Chantiwas, Y.-K. Cho, H. Shin and S. A. Soper, *Analyst*, 2014, **139**.
8. R. Karnik, R. Fan, M. Yue, D. Li, P. Yang and A. Majumdar, *Nano Letters*, 2005, **5**, 943-948.